In situ magnetic measurements under neutron radiation in Fe metal and low carbon steel

S. Takahashi,[a] H. Kikuchi, and K. Ara
Nondestructive Evaluation and Science Research Center, Faculty of Engineering, Iwate University, Morioka 020-8551, Japan

N. Ebine
Department of Reactor Safety Research, Japan Atomic Energy Agency, Tokai, Ibaraki 319-1195, Japan

Y. Kamada and S. Kobayashi
Nondestructive Evaluation and Science Research Center, Faculty of Engineering, Iwate University, Morioka 020-8551, Japan

M. Suzuki
Department of Reactor Safety Research, Japan Atomic Energy Agency, Tokai, Ibaraki 319-1195, Japan

Magnetic minor hysteresis loops of low carbon steel and Fe metal have been measured during neutron radiation at 563 K in a 50 MW nuclear reactor. For investigation of nucleation mechanism of copper precipitates and dislocation loops during neutron radiation, special attention was paid to minor-loop coefficients, which are deduced from simple relations between minor-loop parameters and are very sensitive to lattice defects such as dislocations, copper precipitates, and grain boundaries. We found that with increasing neutron fluence, the minor-loop coefficients of low carbon steel sharply increase and show a maximum at the fluence of 1×10^{19} cm^{-2}, followed by a slow decrease. The appearance of the maximum suggests the presence of two mechanisms of internal stress; while copper precipitates and dislocation loops in the matrix make the internal stress increase, those grown in the vicinity of dislocations compensate the internal stress of dislocations so as to minimize the elastic energy. On the other hand, the minor-loop coefficients show a monotonic increase with neutron fluence in Fe metal where dislocation loops play an important role for the brittleness. © *2006 American Institute of Physics*. [DOI: 10.1063/1.2214214]

I. INTRODUCTION

The change of mechanical properties due to neutron irradiation has been studied for reactor pressure vessel materials and their model alloys.[1] The neutron radiation induces several kinds of lattice defects such as vacancies, interstitial atoms, voids, dislocation loops, and copper precipitates. Some of the lattice defects make the ductility of materials low and make the brittleness increase. The structure of copper precipitates has been studied using an atom-probe field ion microscope[2] and positron annihilation[3] because copper precipitation is the primary cause of brittleness in nuclear reactor pressure vessels (NRPVs). It was revealed that copper precipitates with the size of 2–3 nm, which are nucleated and grown by the irradiation, make materials brittle.[4,5] However, the nucleation mechanism which takes into effect of dislocations has not been studied in detail, although the NRPV has high dislocation density ρ even in the initial state. Dislocations would exert a great influence on the nucleation of lattice defects because there exists the elastic interaction between copper precipitates and dislocations. Our interest is in the nucleation mechanism of copper precipitates during neutron radiation, especially the interaction of radiation defects with dislocations in A533B steel. A533B steel is low

carbon steel (0.19 wt % C, 0.19 wt % Si, 1.47 wt % Mn, 0.16 wt % Cu, 0.64 wt % Ni, 0.51 wt % Mo, 0.14 wt % Cr, balance Fe) and is used in the NRPV.

The lattice defects can be observed directly or indirectly after neutron irradiation; the direct observation is due to a transmission electron microscope (TEM), while the indirect one is due to the magnetic method,[6] the atom-probe field ion microscope,[2] positron annihilation,[3] small angle neutron scattering,[7] electric resistance,[1] etc. The information on radiation defects obtained by these currently employed methods is limited because current methods are used to measure physical properties only before and after the irradiation. The magnetic method has several advantages in getting information on lattice defects and can be technically applied for *in situ* measurements during neutron radiation in the nuclear reactor. The *in situ* observation of lattice defects by magnetic method gives us detailed information about irradiation damages against the neutron fluence. The main purpose of the present study is to perform magnetic measurements under neutron irradiation in the nuclear reactor.

The relationship between magnetism and dislocations in ferromagnetic metals was investigated by the Stuttgart group of Max-Planck Institute.[8] The strain field around dislocations exerts an influence on magnetization hysteresis loops through the magnetoelastic coupling in ferromagnetic metals such as Ni, Fe, and Co metals. The structure-sensitive properties change with the density and distribution of disloca-

[a] Electronic mail: seiki.t@iwate-u.ac.jp

tions. The relationship of magnetic properties with other lattice defects such as vacancies, interstitial atoms, has not been studied in detail so far because these lattice defects bring about only a small change to the hysteresis loops; the size of these lattice defects is too small compared with the width of the magnetic domain wall to disturb the domain wall motion significantly.

Recently, an analysis method of minor hysteresis loops has been found in Fe single crystals, Fe polycrystals, and low carbon steel.[9–12] Minor-loop coefficients deduced from simple relations between parameters of minor loops are independent of the magnetic field amplitude and are much more sensitive to dislocations and grain boundaries than the traditional magnetic properties of the major loop. In addition, one can obtain the minor-loop coefficients with much lower magnetic field compared with that of the major loop. For instance, 1 kA/m is sufficient for minor-loop analysis of A533B steel, though we need more than 10 kA/m for the major loop.[12] Such low field measurements are very useful for present *in situ* magnetic measurements because the maximum applied field is limited to 2 kA/m owing to the limited space of an irradiation capsule for ring core samples.

The other purpose of the present study is to make a database of the relation between minor-loop coefficients and radiation defects. Currently, the integrity of pressure vessels is evaluated by Charpy impact test, which is a destructive testing. The lack of Charpy impact test samples preinstalled in the reactor is an urgent issue. On the other hand, the integrity can be evaluated nondestructively by the magnetic method. The database is necessary for the practical realization of the magnetic method for nondestructive evaluation of NRPV.

Copper precipitates and dislocation loops are main lattice defects that cause the brittleness of NRPV during neutron radiation. In irradiated A533B steel, there coexist copper precipitates and dislocation loops, while only dislocation loops are induced by the radiation in Fe metal. In the present investigation, we studied radiation effects in A533B steel and Fe metal, and tried to separate the effects of these two lattice defects, in order to elucidate the relation between copper precipitates and minor-loop properties. The *in situ* measurements were performed at the same temperature as 563 K of the commercial reactor operation.

II. ANALYSIS METHOD OF MINOR HYSTERESIS LOOPS

To analyze minor hysteresis loops, we introduce minor-loop properties as shown in Fig. 1; minor-loop magnetization M_a^*, minor-loop coercive force H_c^*, minor-loop remanence M_R^*, minor-loop hysteresis loss W_F^*, minor-loop remanence work W_R^*, and minor-loop susceptibilities χ_H^*, χ_R^*, and χ_a^*. These parameters are used to represent characteristics of a set of minor hysteresis loops. They correspond to saturation magnetization M_s, coercive force H_c, remanence M_R, hysteresis loss W_F, remanence work W_R, and susceptibilities, in the major loop, respectively. W_R^* is the area enclosed by a minor loop in the second quadrant. We can obtain information about the potential energy of domain wall displacement by analyzing these minor-loop properties.
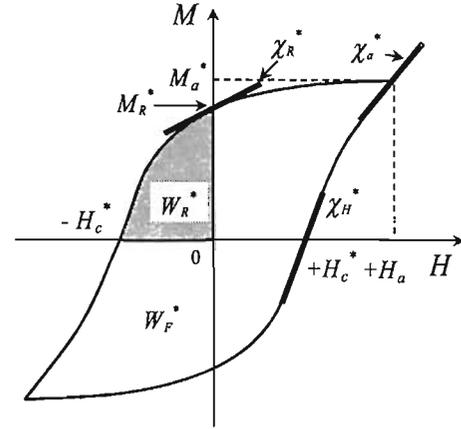
FIG. 1. The magnetic properties of a minor hysteresis loop; magnetic field amplitude H_a, minor-loop coercive force H_c^*, minor-loop magnetization M_a^* at H_a, minor-loop hysteresis loss W_F^*, minor-loop remanence M_R^*, minor-loop remanence work W_R^*, and three minor-loop susceptibilities χ_H^*, χ_R^*, and χ_a^* at $H=H_c^*$, 0, and H_a, respectively.

We found six relations between the minor-loop properties in a set of minor loops, which are independent of the magnetic field amplitude H_a as well as magnetic field.[11,12] In the second stage where Bloch walls mainly contribute to the magnetization, W_F^* and W_R^* have a simple relation with M_a^* and M_R^*, respectively, as follows:

$$W_F^* = W_F^0 \left(\frac{M_a^*}{M_s} \right)^{n_F} \tag{1}$$

and

$$W_R^* = W_R^0 \left(\frac{M_R^*}{M_R} \right)^{n_R}. \tag{2}$$

Here, W_F^0 and W_R^0 are coefficients representing the magnitude and the trough depth of Bloch wall potential, respectively, and are sensitive to lattice defects. n_F and n_R are constants independent of lattice defects as well as the kind of materials: $n_F \sim n_R \sim 3/2$. Note that the power-law relation with $n_F = 1.6$ between W_F^* and M_a^* was discovered by Steinmetz about one century ago and is well-known as the Steinmetz law.[13]

H_c^* corresponds to the height of the crest of potential and M_R^* represents the position of the trough in the vicinity of the crest. It was revealed that H_c^* has a simple relation with M_R^* in the second stage, given by

$$H_C^* = H_C^0 \left(\frac{M_R^*}{M_R} \right)^{n_C}, \tag{3}$$

where H_c^0 is a coefficient representing the height of potential and n_c is a constant which slightly depends on the kind of materials: $n_c \sim 0.45$.

In the initial stage of the magnetization process, three minor-loop susceptibilities χ_H^*, χ_R^*, and χ_a^* are a function of H_c^*, M_R^*, and M_a^*, respectively, and are given by

$$R_C^* = \frac{1}{\chi_H^*} = R_C^0 \exp \left(-b \frac{H_C^*}{H_C} \right), \tag{4}$$
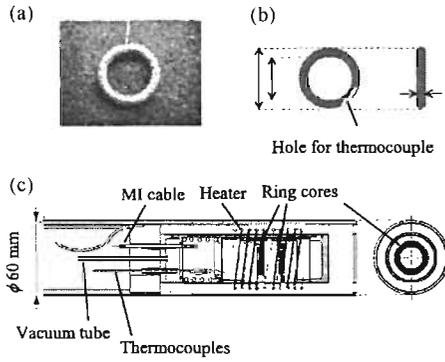
FIG. 2. (a) Photograph and (b) size of a ring core sample. (c) Part of irradiation capsule equipped with ring cores.

$$\chi_R^* = \chi_T^0 \left(\frac{M_R^*}{M_R} \right)^{n_T},$$

(5)

and

$$\chi_a^* = \chi_s^0 \left(\frac{M_a^*}{M_s} \right)^{n_s}.$$

(6)

Here, R_c^0, χ_T^0, and χ_s^0 are coefficients which represent the resistance at the crest, the mobility at the trough, and the averaged mobility of Bloch wall, respectively. b, n_T, and n_s are constants which depend on the kind of materials, and have a value of 2–6, 0.1–0.5, and 0.5–1.0, respectively.

All minor-loop coefficients are sensitive to lattice defects compared with the structure-sensitive properties of the major loop and have a proportional relation with coercive force.[12] In the present study, the relations of Eqs. (1)–(6) which were obtained in plastically deformed Fe metal and A533B steel were adapted to the investigation of the effect of neutron radiation on minor-loop properties in Fe metal and A533B steel.

III. EXPERIMENTAL PROCEDURE

Sheet samples of Fe polycrystals with purity of 99.99% and A533B steel were prepared by cold rolling. During the manufacturing process, the steel was austenitized by aging at 1153 K for 1 h and was tempered at 943 K for 80 min for the formation of bainite structure. The samples were shaped into a ring core with electric discharge machine for magnetic measurements as shown in Figs. 2(a) and 2(b).

Magnetic measurements of ring cores under neutron radiation were performed in Japan Material Testing Reactor at Japan Atomic Energy Agency. For *in situ* magnetic measurements, the ring cores with an exciting coil, pickup coil, and thermocouple, were installed into an irradiation capsule as shown in Fig. 2(c). Mineral insulated (MI) cables which have high durability against neutron irradiation were used for the coils. The MI cable with a diameter of 0.5 mm comprises a copper wire for the exciting coil, a constantan wire for the pickup coil, MgO insulator, and a stainless steel sheath. This wire was also used for thermocouples because of the high durability against neutron irradiation. This MI cable was wound on the ring core with 100 turns, which yields a maximum applied field of 2 kA/m. The MI cables extended from
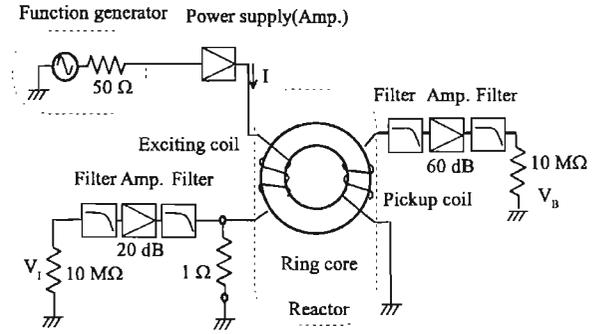
FIG. 3. Schematic diagram of electric circuit for minor-loop measurements.

the capsule were connected to an electronic circuit installed outside the reactor.

Figure 3 shows a schematic diagram of the electronic circuit for minor-loop measurements. A triangular voltage from a function generator was applied to a bipolar power supply. The bipolar power supply converts voltage to current and amplifies the current. The amplified current was applied to the exciting coil to magnetize the ring cores with a rate of $400 \ A \ m^{-1} \ s^{-1}$. The magnetic field inside the ring cores was obtained from the voltage V_I across an $1 \ \Omega$ resistance connected to the exciting coil in series. The induced voltage of the pickup coil was purified by a low pass filter with cutoff frequency of 30 Hz, then amplified with gain of 60 dB, and filtered again. After these signal processing, the induced voltage V_B was integrated to obtain the magnetic flux inside the ring cores. A set of minor hysteresis loops were measured by increasing the amplitude of wave current gradually.

For the *in situ* magnetic measurements at 563 K, the temperature of samples was first increased from 300 to 423 K without neutron radiation in the rate of 0.2 K/min. The reactor power was then increased from 0 to 50 MW with a rate of 0.5–1.0 MW/min and the temperature was increased from 423 to 563 K in the rate of 14 K/min. The neutron flux was approximately $0.5 \times 10^{13} \ cm^{-2} \ s^{-1}$ and the total neutron fluence was $5 \times 10^{19} \ cm^{-2}$. *In situ* magnetic measurements were carried out every three or four days at the reactor power of 50 MW. The temperature of samples was monitored with the thermocouples inserted into the samples. The temperature of A533B steel and iron metal samples was stabilized at 562 ± 1.5 K and 563 ± 1 K, respectively, by using a heater and regulating the helium pressure in the capsule.

IV. EXPERIMENTAL RESULTS

A. Temperature dependence of minor-loop coefficients

In the previous study,[12] the relations of Eqs. (1)–(6) were examined experimentally at room temperature for plastically deformed A533B steel. Minor-loop coefficients, W_F^0, W_R^0, H_c^0, R_c^0, χ_T^0, and χ_s^0 have a good relation with true stress which corresponds to the residual internal stress due to dislocations. In this study, the *in situ* measurements in the nuclear reactor has been carried out at a higher temperature of 563 K. Therefore, we first checked the temperature dependence of minor-loop coefficients in our laboratory before *in*
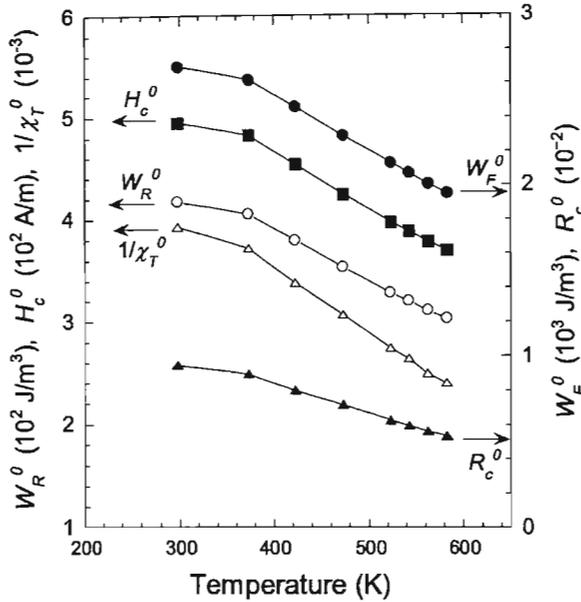
FIG. 4. Minor-loop coefficients, W_F^o, W_R^o, H_c^o, R_c^o, and $1/\chi_T^o$, as a function of temperature in A533B steel.

situ measurements in the nuclear reactor. A set of minor loops was measured isothermally by using a flux meter in the temperature range from 300 to 583 K. It was found that all minor-loop constants n_F, n_R, n_c, b, and n_T are independent of temperature, and are 1.48, 1.43, 0.28, 3.4±0.3, and 0.13±0.01, respectively. These values are consistent with those of plastically deformed A533B steels. As shown in Fig. 4, the minor-loop coefficients, W_F^o, W_R^o, H_c^o, R_c^o, and $1/\chi_T^o$ decrease monotonically with increasing temperature from 300 to 583 K. The decreasing rate of W_R^o, W_F^o, and H_c^o at 563 K is about 0.15%/K, while that of R_c^o and $1/\chi_T^o$ is about 0.24%/K. These results were also obtained in the present *in situ* magnetic measurements in the nuclear reactor. Note that since χ_a^* includes a large experimental error, the result of χ_s^o is omitted in this study.

B. Minor-loop coefficients under neutron radiation

The temperature of A533B steel sample was controlled automatically within 562±1.5 K throughout the radiation experiment. This yields a maximum deviation of 0.2% in W_R^o, W_F^o, and H_c^o, 0.5% in R_c^o, and $1/\chi_T^o$ from the value at T =562 K. Although this deviation did not change the fluence dependence of minor-loop coefficients significantly, the data were corrected for the temperature deviation to obtain an accurate value of the coefficients at T=562 K. It should be noted that temperature rise due to heat radiation of exciting coils during minor-loop measurements does not affect experimental results, because the data below 0.8 kA/m were used for the minor-loop analysis and the rise of temperature was less than 0.5 K.

Dependence of minor-loop coefficients on neutron fluence in Fe metal was obtained by analyzing a set of minor loops with Eqs. (1)–(6). Figure 5 shows minor-loop coefficients W_F^o, W_R^o, and H_c^o as a function of neutron fluence in Fe metal. One can see that all coefficients increase monotonically with the increase of neutron fluence. Their increase
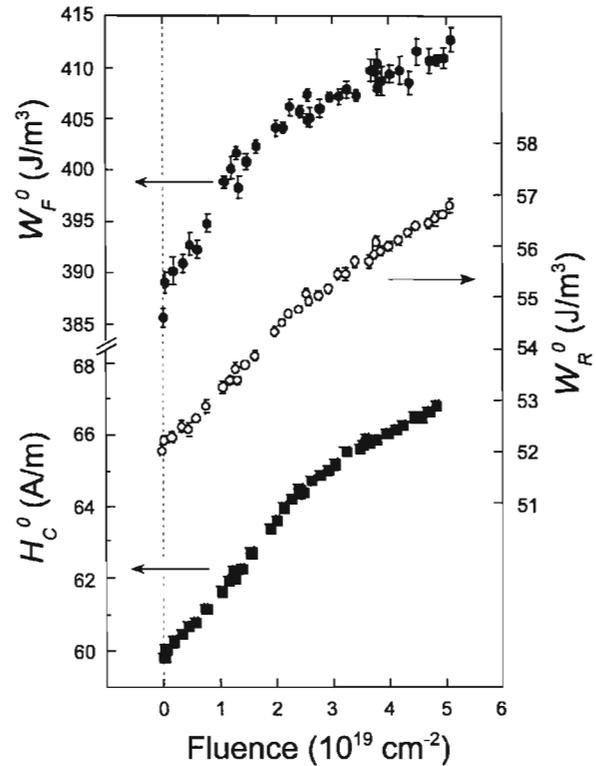
FIG. 5. Neutron fluence dependence of W_F^o, W_R^o, and H_c^o in Fe metal.

corresponds to the increase of stress field and is consistent with the fact that the irradiation damage increases during neutron radiation.[1]

However, in A533B steel, the dependence of minor-loop coefficients on neutron fluence is largely different from that of Fe metal. As shown in Fig. 6, minor-loop coefficients W_F^o,
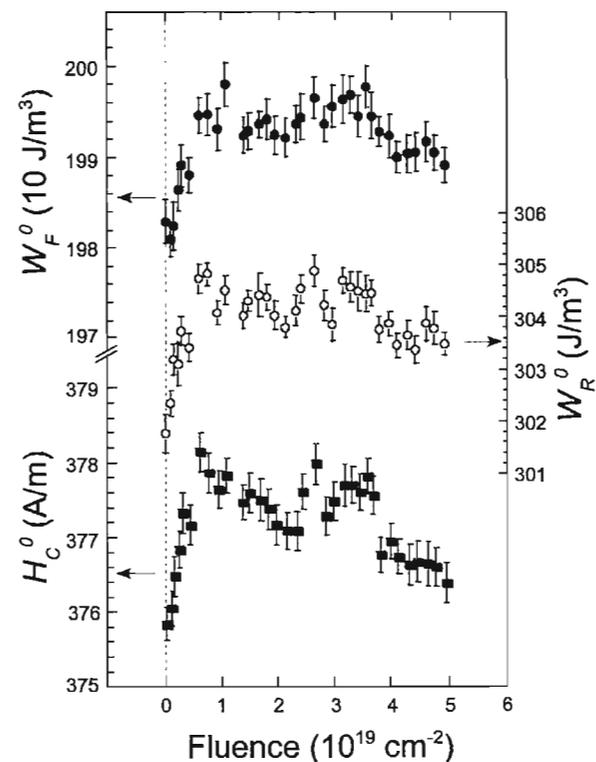
FIG. 6. Neutron fluence dependence of W_F^o, W_R^o, and H_c^o in A533B steel.
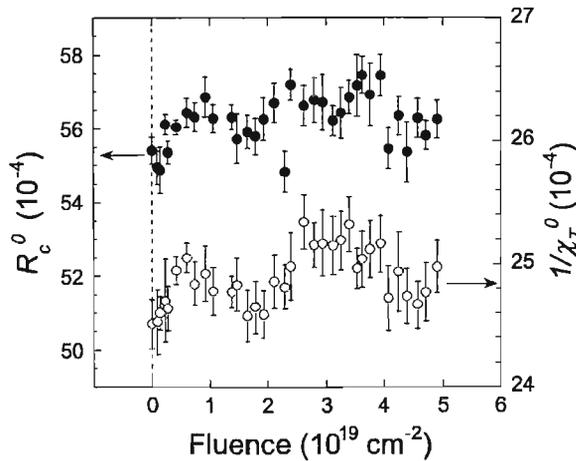
FIG. 7. Neutron fluence dependence of R_c^o and $1/\chi_T^o$ in A533B steel.

W_R^o, and H_c^o sharply increase due to the radiation and show a maximum at the fluence of 1×10^{19} cm^{-2}. With increasing the neutron fluence, these coefficients slowly decrease and seem to have another local maximum around 3×10^{19} cm^{-2}. As shown in Fig. 7, such maxima were observed also for $1/\chi_T^o$, although the maximum around 3×10^{19} cm^{-2} was not clearly seen for R_c^o. The maximum of minor-loop coefficients at the initial stage of neutron irradiation has been observed also in Fe model alloys after neutron irradiation.[14] The decrease of the minor-loop coefficients indicates that the irradiation damage decreases above 1×10^{19} cm^{-2}, contrary to the results of Fe metal.

V. DISCUSSION

The minor-loop coefficients are a function of modulus of rigidity, Poisson ratio, magnetostriction constant, and magnetic anisotropy constant, and their temperature dependence gives us information on their functional structure. As shown in Fig. 4, all coefficients decrease linearly with temperature and show a similar temperature dependence. Therefore, the minor-loop coefficients would have a similar functional structure of such physical properties.

Minor-loop coefficients W_F^o, W_R^o, and H_c^o are sensitive to the size and shape of Bloch wall potential, while those related to susceptibilities, R_c^o, $1/\chi_T^o$ and $1/\chi_s^o$, depend on the resistance against the movement of Bloch wall at the special point of potential. Generally, the coefficients are sensitive to dislocations because of magnetoelastic interaction between domain walls and dislocations.[8] The minor-loop coefficients also give information about irradiation damage due to other lattice defects such as copper precipitates and dislocation loops, because these defects also yield stress field around them.

In Fe metal, all minor-loop coefficients W_F^o, W_R^o, and H_c^o increase monotonically during neutron radiation as shown in Fig. 5. The irradiation damage in Fe metal would be due to dislocation loops, vacancies, and interstitial atoms. Since the size of vacancies and interstitial atoms are too small to exert an influence to Bloch wall motion, only dislocation loops would play an important role for obstacles to the Bloch wall motion in Fe metal. The number and size of

dislocation loops increase with the increase of neutron fluence, resulting in the monotonic increase in the minor-loop coefficients. On the other hand, in A533B steel, minor-loop coefficients increase during neutron radiation and show a maximum at the fluence of 1×10^{19} cm^{-2}, followed by a slow decrease with neutron fluence. This change in the minor-loop coefficients indicates that the residual internal stress decreases and obstacles to the Bloch wall motion become small above the fluence of 1×10^{19} cm^{-2}.

The metallurgical differences between A533B steel and Fe metal are chemical compositions and the value of ρ; the value of ρ for A533B steel is above 3×10^{10} cm^{-2} and is much higher than the value of Fe metal.[15] The radiation defects that yield the brittleness in A533B steel would be copper precipitates and dislocation loops, since they act as obstacle to the dislocation movement. Copper precipitates and dislocation loops do not diminish with the increase of neutron fluence eventhough the density of such defects is saturated at a high fluence.

Generally, mechanical properties such as yield stress, Vickers hardness, and ductile-brittle transition temperature (DBTT) increase with neutron fluence for all materials. It was confirmed for present A533B steel that both Vickers hardness and DBTT increase after neutron irradiation with the fluence of 5×10^{19} cm^{-2}. Such a change of mechanical properties can be explained by the dislocation theory and is contradictory to the minor-loop properties in A533B steel.

The maximum of minor-loop coefficients in A533B steel would be explained by the introduction of an idea that copper precipitates grow in the vicinity of dislocations by neutron irradiation. Copper precipitates and dislocation loops in the matrix have stress field in themselves and make the minor-loop coefficients increase. On the other hand, the stress field is reduced and minor-loop coefficients decrease when these two lattice defects exist in the vicinity of dislocations. Edge dislocations include the compressive and repulsive stress field, and both dislocation loops and copper precipitates may gather around the dislocations through the elastic interaction. Both radiation defects will compensate the stress field of dislocations and this compensation brings about a reduction in the elastic energy. The emulation of these two effects of stress field in the matrix and around dislocations would result in the maximum of minor-loop coefficients. These radiation defects fixed around dislocations strongly disturb the dislocation movement and make mechanical properties increase as was observed experimentally.

In the same way, dislocation loops nucleate and grow during neutron radiation, also in Fe metal. However, dislocation density before neutron radiation, estimated from coercive force of 60 A/m, is 7×10^8 cm^{-2} and is very small compared with that of A533B steel. Therefore, the stress field of dislocations may be compensated partially by dislocation loops and the net stress field increases during neutron radiation.

Quite recently, small dislocation loops and copper precipitates in the vicinity of dislocations have been observed

by TEM in A533B steel after neutron irradiation with the fluence of 5×10^{19} cm^{-2}. The density of dislocation loops and copper precipitates in the vicinity of the dislocations was found to be higher than that in the matrix. The results by TEM observation will appear in a separate paper.

VI. CONCLUSION

In situ magnetic measurements have been successfully carried out under neutron radiation at 563 K. We found that the nucleation mechanism of radiation defects in Fe metal and A533B steel is largely different from each other.

In Fe metal, minor-loop coefficients increase monotonically with the increase of neutron fluence. Dislocation loops which nucleate and grow during neutron radiation, make the minor-loop coefficients increase through magnetoelastic coupling.

On the other hand, in A533B steel, the minor-loop coefficients increase initially and show a maximum at the neutron fluence of 1×10^{19} cm^{-2}, followed by a slow decrease with neutron fluence. This indicates the presence of two mechanisms of internal stress due to radiation defects in A533B steel. The copper precipitates and dislocation loops gathering in the vicinity of dislocations would disturb the dislocation movement and make A533B steel brittle.

[1] J. Koutský and J. Koík, *Radiation Damage of Structural Materials* (Elsevier Science, New York, 1994).
[2] P. Othen, M. Jenkins, G. Smith, and W. Phythian, Philos. Mag. Lett. **64**, 383 (1991).
[3] S. Pizzini, K. Roberts, W. Phythian, C. English, and G. Greaves, Philos. Mag. Lett. **61**, 223 (1990).
[4] A. Youle and B. Ralph, Met. Sci. J. **6**, 149 (1972).
[5] S. Goodman, S. Brenner, and J. R. Low, Jr., Metall. Trans. **4**, 2371 (1973).
[6] I. Altpeter, G. Dobmann, K.-H. Katerbau, M. Schick, P. Binkele, P. Kizler, and S. Schmauder, Nucl. Eng. Des. **206**, 337 (2004).
[7] M. K. Miller, B. D. Wirth, and G. R. Odette, Mater. Sci. Eng., A **353**, 133 (2003).
[8] H. Kronmüller and M. Fähnle, *Micromagnetism and the Microstructure of Ferromagnetic Solids* (Cambridge University Press, Cambridge, 2003).
[9] S. Takahashi, L. Zhang, and T. Ueda, J. Phys.: Condens. Matter **15**, 7997 (2003).
[10] S. Takahashi, T. Ueda, and L. Zhang, J. Phys. Soc. Jpn. **73**, 239 (2004).
[11] S. Takahashi and L. Zhang, J. Phys. Soc. Jpn. **73**, 1567 (2004).
[12] S. Takahashi, L. Zhang, S. Kobayashi, Y. Kamada, H. Kikuchi, and K. Ara, J. Appl. Phys. **98**, 033909 (2005).
[13] C. P. Steinmetz, *Theory and Calculation of Electric Circuits* (McGraw-Hill, New York, 1917).
[14] S. Kobayashi, H. Kikuchi, S. Takahashi, K. Ara, Y. Kamada (unpublished).
[15] S. Takahashi, J. Echigoya, and Z. Motoki, J. Appl. Phys. **87**, 805 (2000).